-RESEARCH PAPER-

International Journal of Mining and Geo-Engineering

IJMGE

IJMGE 60-3 (2026) 367-377

DOI: 10.22059/IJMGE.2026.419137.595411

Effects of ore types and blending strategy on the flotation performance, using igneous phosphate ore from Esfordi deposit

Mohammad Dehghani [a], Hassan Maleki [a], Yasamanzahra Alishahiha [a], Mohammad Noaparast [a,*] and Golnaz Jozanikohan [a]

[a] *School of Mining Engineering, College of Engineering, University of Tehran, Tehran, Iran.*

Article History:

Received: 22 July 2026.

Revised: 04 September 2026.

Accepted: 25 September 2026.

ABSTRACT

The Esfordi deposit, Iran's largest igneous phosphate resource, exhibits significant mineralogical heterogeneity that causes feed quality fluctuations and compromised flotation performance. This study presents the first systematic comparison of two mineralogically distinct ore types from this deposit: an iron-rich apatite ore (P1) and a clay-bearing green phosphate ore (P2). Feed blending was then evaluated as a practical strategy for managing this ore variability. Mineralogical characterization revealed that P1 contained 13.86% P_2O_5 and 47.17% Fe_2O_3, whereas P2 assayed 10.72% P_2O_5 and 16.55% Fe_2O_3 and contained 10.6% clay minerals. Flotation conditions were optimized through systematic studies of collector dosage, pH, starch dosage, and cleaning stages following desliming. Under optimized conditions (pH 9.5 and 400 g/t starch), P1 achieved a concentrate grade of 40.81% P_2O_5 and 80.53% recovery, using only 280 g/t collector—down from the current plant practice of 680 g/t, a 59% reduction. In contrast, P2 required 680 g/t collector and yielded 31.05% P_2O_5 with 71.38% recovery, due to increased reagent consumption associated with clay minerals. Among the tested blending ratios, the 70:30 (P1:P2) blend provided the most favorable balance, producing a concentrate containing 35.26% P_2O_5 and 2.08% Fe_2O_3 with 63.82% recovery while reducing collector consumption by 32% relative to P2 alone. These findings demonstrated that feed blending can effectively mitigate the adverse effects of ore type, maintain concentrate quality, and reduce reagent requirements. Adjusting blending ratios and reagent dosage according to feed characteristics can improve flotation performance and provide practical guidance for plant operation.

Keywords: *Igneous phosphate ore; Apatite flotation; Ore variability; Blending; Flotation optimization.*

1. Introduction

Phosphorus is an essential, non-substitutable nutrient for global agriculture, and phosphate rock remains the principal source of phosphoric acid and fertilizer products worldwide [1]. Global P_2O_5 demand continues to rise, driven by agricultural intensification in Asia and South America [2], and while world phosphate resources are conventionally divided into sedimentary phosphorites (~95%) and igneous deposits (~5%) associated with carbonatite and alkaline intrusive complexes, igneous ores generally yield purer concentrates after beneficiation owing to simpler, silicate- and iron-oxide-dominated gangue assemblages rather than the clay-rich matrices typical of sedimentary phosphorites [1].

Beneficiation of both ore types relies overwhelmingly on froth flotation [3] to upgrade run-of-mine material to fertilizer-grade concentrates. Two general strategies are applied: direct (anionic) flotation, in which apatite is floated using fatty-acid collectors while silicate and carbonate gangue are depressed, and reverse (double) flotation, in which siliceous gangue is floated first with cationic amines near neutral pH, followed by carbonate removal under acidic conditions, leaving phosphate in the non-floated fraction [4, 5, 6]. The choice between routes depends largely on gangue mineralogy—siliceous and iron-oxide-bearing in most igneous ores, versus carbonate- and collophane-rich in many sedimentary phosphorites [7, 8].

The flotation behaviour of apatite is governed by its semi-soluble, calcium-bearing surface, which shares electrochemical similarities with calcite, dolomite, and fluorite, making selective separation intrinsically difficult [9, 10, 11]. Water chemistry and dissolved ionic species further modify apatite floatability [12], and rare-earth-element enrichment at apatite surfaces has additional relevance to beneficiation behaviour [13]. Sodium oleate and other fatty acid collectors remain the industry standard owing to strong collecting power despite limited selectivity [4]; mechanistic studies using FTIR, zeta-potential, and XPS techniques show that oleate adsorbs through chemisorption at surface calcium sites, and at higher concentrations, surface precipitation of calcium oleate [14, 15, 16]. This calcium-mediated mechanism also promotes non-selective activation of gangue minerals, motivating recent work on more selective depressants such as gallic acid [17], and on modified collector chemistries—amide derivatives, dicarboxylate reagents, surfactant mixtures, and vegetable-oil-based soaps—aimed at improving apatite–gangue differentiation [18-22]. For iron-oxide gangue specifically, oleate–hematite interactions are non-trivial, exhibiting a recovery minimum under alkaline conditions and adsorption behaviour sensitive to particle fineness [23, 24]. Collectively, these studies indicate that interfacial regulation—jointly optimizing collector adsorption, depressant selectivity, and reagent dosage—remains the central scientific challenge in apatite flotation [9].

Particle size and mineral liberation exert a further, first-order control on flotation performance. Recovery is maximized within an intermediate size range, declining sharply for both ultrafine particles,

* Corresponding author: *E-mail address:* Noparast@ut.ac.ir (M. Noaparast).

owing to poor bubble–particle collision efficiency, and coarse particles, owing to bubble–particle detachment under turbulence [25, 26]; in reverse phosphate flotation specifically, the presence of fines has been shown to alter apatite–dolomite separation behaviour [27]. Classical liberation-based characterization methods remain relevant to interpreting such size-dependent responses [28].

Beyond particle-scale effects, ore variability at the deposit scale is increasingly recognized as a major, often underappreciated, determinant of plant performance. Geometallurgical characterization of the Lappberget polymetallic deposit demonstrated that flotation selectivity and recovery vary substantially across mineralogically and texturally distinct domains within a single ore body [29, 30], and that blending ratios of distinct ore units can alter recovery, mass pull, and concentrate grade in non-additive ways [29]. Comparable evidence exists within the phosphate literature itself where flotation parameters optimized for one ore type have been shown not to transfer directly to another of differing geological origin [31]. Predictive and blending-oriented approaches of this kind, however, have been developed mainly for base-metal sulfide systems; their extension to igneous phosphate ores—where variability can arise from differing degrees of hydrothermal alteration, apatite generation, and gangue assemblage—remains comparatively unexplored.

Reagent selection for both sedimentary and igneous Iranian phosphate ores has recently been examined directly, including the systematic comparison of collector–depressant systems for the reverse flotation of apatite and collophane from a sedimentary phosphate ore sample [32]. This work illustrates that the interaction between collector type, depressant selection, and gangue mineralogy identified in the broader literature [9–24] is equally decisive for Iranian phosphate ores, and that reagent optimization cannot be generalized across ore types without direct comparative testing.

The Esfordi deposit, in the Bafq metallogenic province of Yazd Province, central Iran, is the country's principal igneous phosphate producer and one of the most extensively studied Kiruna-type apatite–magnetite deposits [33, 34]. It is hosted by Early Cambrian rhyolitic volcanics intercalated with carbonate sediments, with apatite occurring in at least two generations—an early magmatic, crystalline form associated with magnetite, and a later, amorphous-to-microcrystalline form of probable hydrothermal-to-supergene origin [33, 35-37]. This mineralogical duality has direct metallurgical significance, since apatite generations of differing crystallinity and gangue association can be expected to respond differently to flotation reagents even at similar bulk P_2O_5 grade. The Esfordi concentrate additionally carries monazite and xenotime as REE hosts alongside apatite, with implications for downstream processing [38]. Previous process-metallurgy work at Esfordi has focused on optimizing rougher flotation parameters—collector and depressant dosage, pH, and conditioning time [39]—and on the general operating-parameter dependence of apatite flotation [7], but has treated the plant feed as a single, statistically homogeneous ore. In this matter, there is no prior study which has systematically compared the flotation response of distinct, mineralogically defined ore types from within the Esfordi deposit, nor evaluated blending of such ore types as a deliberate strategy for managing feed variability—an approach already shown to be valuable in base-metal geometallurgy [29, 30] but not yet transferred to igneous phosphate processing.

This gap matters for two reasons. First, as reviewed above, gangue mineralogy, particle size, liberation, and degree of alteration could of course strongly influence flotation response [1, 9, 25, 29, 31], and Esfordi is known to host genuinely distinct ore populations rather than a single homogeneous type [33, 35]. Reagent schemes optimized for one ore type may therefore be suboptimal for another as mining progresses through zones of differing mineralogy. Second, processing plants rarely handle a single ore type in isolation; feed blending is standard practice, yet the metallurgical response of blends cannot always be predicted from the additive behaviour of their constituent ore types [29]. Whether blending can serve as a practical tool for managing ore variability at Esfordi remains untested. The present study addresses this gap through the comparative evaluation of flotation behaviour of two mineralogically distinct ore types from the Esfordi deposit and the assessment of feed blending as a strategy for managing ore variability. This dual focus distinguishes the present work from earlier Esfordi-specific studies which optimized reagent and operating conditions for a single, generalized feed, and extends the ore-type-resolved, comparative collector–depressant approach recently applied to a sedimentary Iranian phosphate ore [32] to an igneous deposit, where the underlying sources of variability differ fundamentally.

Accordingly, the objectives of this study are: i) to characterize the mineralogical and textural differences between two representative ore types from the Esfordi deposit; ii) to determine optimal flotation conditions collector and depressant type and dosage, pulp pH, particle size, and conditioning time independently for each ore type; iii) to quantify and compare the resulting P_2O_5 grade, recovery, and gangue rejection between the two ore types under their respective optimized conditions; and iv) to evaluate the metallurgical response of blended feeds at varying blend ratios, assessing the feasibility of feed blending as a practical strategy for managing ore variability at the Esfordi plant.

2. Materials & methods

2.1. Ore samples and preparation

Two phosphate ore samples representing the major ore types of the Esfordi phosphate deposit, Yazd province, central Iran, were supplied and used in this study. Sample P1 was collected from the iron-apatite horizon, whereas sample P2 was obtained from the green phosphate horizon. The chemical composition of the samples, determined by XRF analysis, is presented in Table 1. The as-received samples were crushed using a jaw crusher to below 3.35 mm, followed by dry grinding in a laboratory rod mill to achieve a d_{80} of approximately 100 µm, as determined by liberation degree analysis. The particle size distribution was measured by wet sieving.

2.2. Mineralogical characterization and liberation degree analysis

Mineralogical studies were performed on polished thin sections using optical microscopy under transmitted and reflected light. Photomicrographs of representative sections are shown in Figure 1. The degree of apatite liberation was determined by point counting approach on size fractions ranging from −2380+1000 µm down to −75 µm. The optimal liberation size was defined as the size at which at least 80% of apatite particles were fully liberated (>95% apatite by volume).

Sample P1: Microscopic examination revealed that opaque minerals, mainly iron oxides, constituted approximately 45–50% of the sample. Hematite was the dominant iron oxide, accounting for about 95% of the iron oxides, occurring as granular and occasionally prismatic to bladed forms (specularite). Magnetite was present as a minor phase (1–2% of iron-bearing minerals), and minor goethite (<1%) was also observed as a result of iron alteration. Transparent minerals included apatite (approximately 12–14%), quartz, calcite, and minor amounts of amphibole and feldspar. Apatite occurred as euhedral crystals, brecciated fragments, and within carbonate veinlets. Inclusions of high-relief particles, likely REE-bearing minerals (approximately 0.1–0.01%), were observed within apatite crystals. Liberation analysis showed that apatite liberation exceeded 80% at particle sizes below 100 µm.

Sample P2: Microscopic studies indicated that iron oxides constituted approximately 10–15% of the sample. Magnetite was the primary iron oxide (70–75% of iron oxides), with hematite (25–30%) and minor goethite also present. Hematite was mainly derived from magnetite alteration. The transparent minerals comprised apatite (approximately 15–17% in coarse fractions, increasing to 45–50% in fine fractions), quartz, calcite, amphibole (tremolite-actinolite), and significant amounts of clay minerals (predominantly montmorillonite). Other minerals included clinopyroxene, talc, and minor epidote. Apatite occurred as coarse fragments and fine grains within the brecciated matrix. Inclusions of high-relief particles (likely REE-bearing minerals) were observed within apatite crystals, mostly finer than 20 µm. Liberation analysis showed that apatite liberation degree exceeded 80% at particle sizes finer than 100 µm.

Table 1. XRF analysis results of ore samples.

Sample	P_2O_5 (%)	Fe_2O_3 (%)	SiO_2 (%)	CaO (%)	MgO (%)	Al_2O_3 (%)
P1	13.86	47.17	19.19	19.71	1.24	1.83
P2	10.72	16.55	30.52	26.38	4.96	3.46

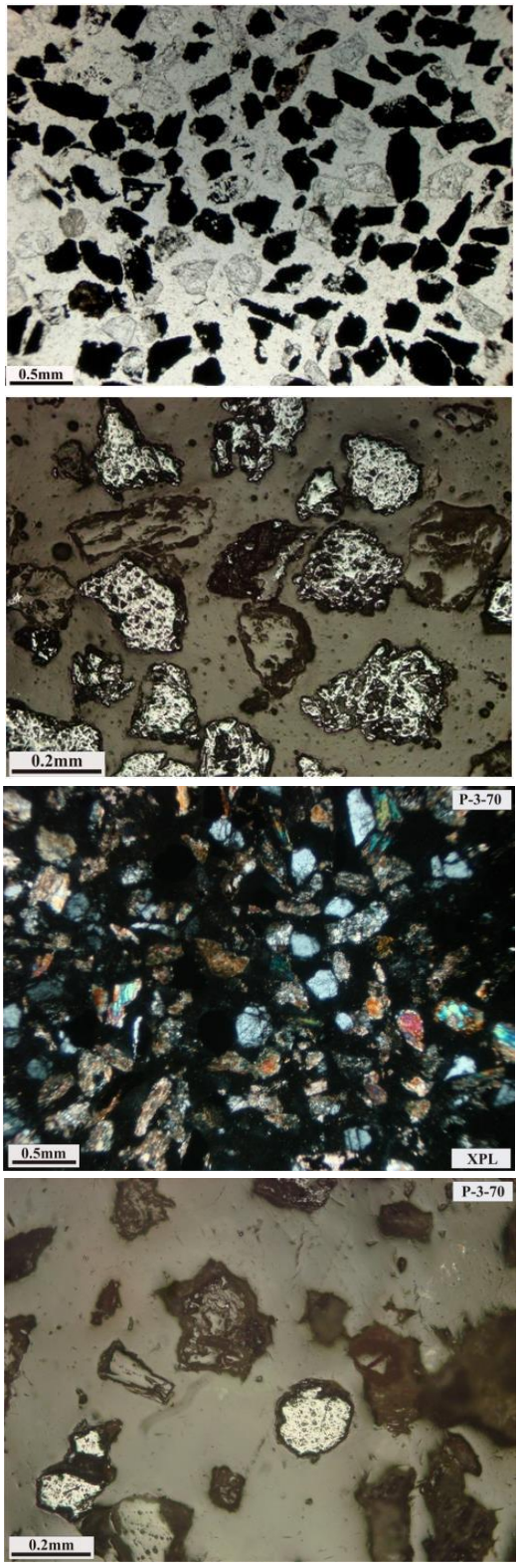

Figure 1. Photomicrographs of thin and polished sections: (A) thin section of P1 (−210+300 µm); (B) polished section of P1 (−210+300 µm); (C) thin section of P2 (−210+300 µm; (D) polished section of P2 (−210+300 µm).

2.3. X-ray diffraction analysis

Semi-quantitative XRD analysis was performed to determine the bulk mineralogy of the two ore types. The results are presented in Table 2. For sample P1, the major minerals were apatite (35.6%), hematite (39.5%), quartz (17.8%), and calcite with dolomite (7.1%). For sample P2, the mineral assemblage comprised apatite/hydroxyapatite (30.3%), actinolite (18.2%), microcline (18.2%), montmorillonite (10.6%), quartz (9.1%), calcite (9.1%), and magnetite (4.5%). The presence of montmorillonite in P2 is particularly significant, as clay minerals are known to increase reagent consumption, and adversely affect flotation performance. The XRD results are consistent with the microscopic studies, confirming the distinct mineralogical differences between the two ore types.

Table 2. Semi-quantitative mineralogical composition of the ore samples determined by XRD analysis.

Mineral	Sample P1 (%)	Sample P2 (%)
Apatite / Hydroxyapatite	35.6	30.3
Hematite	39.5	–
Magnetite	–	4.5
Quartz	17.8	9.1
Calcite / Dolomite	7.1	9.1
Actinolite	–	18.2
Microcline	–	18.2
Montmorillonite	–	10.6

2.4. Desliming procedure

Desliming tests were carried out using a laboratory hydrocyclone (D=50 mm) at feed pressures of 0.5, 0.7, and 1.0 kg/cm². For each test, approximately 5 kg of ground sample at 15% solids was processed. The overflow (slimes) and underflow (deslimed feed) were collected, filtered, dried, weighed, and assayed by XRF. The optimum pressure was selected based on flotation performance.

A lower pressure of 0.3 kg/cm² was not tested because preliminary trials indicated excessive slime loss and unstable cyclone underflow below 0.5 kg/cm²; the tested range (0.5–1.0 kg/cm²) therefore bracketed the practical operating window for the laboratory hydrocyclone used. The mass balance obtained at each pressure, used to justify selection of 0.5 kg/cm², is summarized in Table 3.

2.5. Flotation experiments

Flotation tests were performed in a 1.0 L Denver D-12 mechanical cell type at 1200 rpm. For each test, 500 g of deslimed sample was conditioned in tap water at the desired pulp density (20–35% solids). Reagent additions and conditioning times were as follows:

- Starch (commercial corn starch, 5% w/w solution): 7 minutes conditioning
- Collector (Flo-YS20 + Lina Z80 at ~13% of Flo-YS20): 5 minutes conditioning
- Rougher flotation: 5 min (air flow: 5 L/min)
- Cleaning stages (1 or 2 stages): 3 minutes each, without additional reagents; pulp pH was not re-adjusted during cleaning and was observed to remain within 0.1–0.2 pH units of the rougher value of 9.5, owing to the short duration and residual alkalinity of the rougher pulp.

The parameters investigated were: collector dosage (150–700 g/t), starch dosage (0–500 g/t), pH (8.5–10.5), and pulp density (20–35% solids). After optimizing individual ore types, blended feeds (50:50 and 70:30 P1:P2) were tested under optimized conditions. All tests were performed in duplicate; standard deviations were ±0.5% for grade and ±1.5% for

recovery. Product streams were filtered, dried at 105 °C, weighed, and assayed by XRF.

3. Results

3.1. Preliminary flotation tests (with and without desliming)

Preliminary flotation experiments were conducted to evaluate the effect of desliming on flotation performance, and to select the most suitable reagent system for subsequent optimization tests. These tests were performed on sample P1 using various collector and depressant systems, with and without desliming. The results are summarized in Table 4.

Tests without desliming (Tests 1–10): All tests achieved high recoveries (>97%) but required significantly longer froth collection times. The Flo-YS20 + Lina Z80 system outperformed ALKE + Dirol, yielding higher P_2O_5 grades (30.64–32.41% vs. 28.84–29.66%) and lower Fe_2O_3 grades (11.88–15.84% vs. 18.92–20.76%). Starch was more effective than sodium silicate for iron oxide depression, as indicated by lower Fe_2O_3 grades in the concentrate (11.88–15.84% vs. 17.05–21.77%). This is consistent with the known affinity of starch for iron oxide surfaces through hydrogen bonding which prevents collector adsorption [7, 8].

Tests with desliming (Tests 11–13): Desliming improved the concentrate grade to 34.76–35.86% P_2O_5 and reduced Fe_2O_3 to 8.99–11.14%, although overall recovery decreased to 83.03–87.06% due to phosphate loss in the slimes (6.63–10.16 wt.%). Among the desliming pressures tested, 0.5 kg/cm² produced the highest concentrate grade (35.86% P_2O_5) with the lowest Fe_2O_3 (8.99%), and was therefore selected for subsequent tests.

Oleic acid (Test 14) produced lower P_2O_5 grade (31.74%) and higher Fe_2O_3 (16.98%) compared to the plant collector system. Based on these results, the Flo-YS20 + Lina Z80 collector system and starch depressant were selected for subsequent optimization tests at 0.5 kg/cm² desliming pressure.

3.2. Desliming optimization

Based on the improved performance observed in preliminary tests with desliming, a systematic optimization of hydrocyclone operating pressure was conducted. The effect of feed pressure (0.5, 0.7, and 1.0 kg/cm²) on desliming performance for sample P1 is presented in Figures 2–4. As shown in Figure 2, the weight percentage of slimes increased with decreasing hydrocyclone pressure, from 6.63% at 1.0 kg/cm² to 10.16% at 0.5 kg/cm². Correspondingly, P_2O_5 recovery in the underflow decreased with decreasing pressure (Figure 3), as more phosphate-bearing material was lost to the slimes. Figure 4 shows that the slime fraction consistently contained higher P_2O_5 grade (17.91–18.99%) than the underflow (13.48–13.94%) at all pressures, confirming that apatite is softer and preferentially reports to the fine fraction. This is consistent with the mineralogical characteristics of the ore, where apatite is more friable than the associated iron oxides.

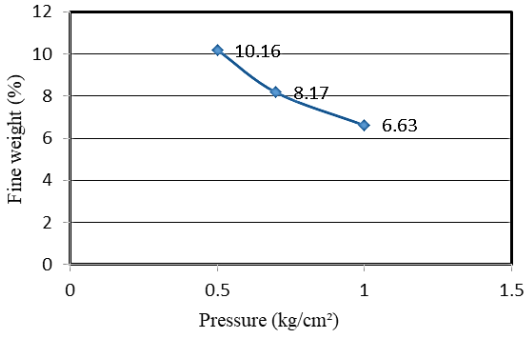

Figure 2. Effect of hydrocyclone pressure on slimes weight percentage.

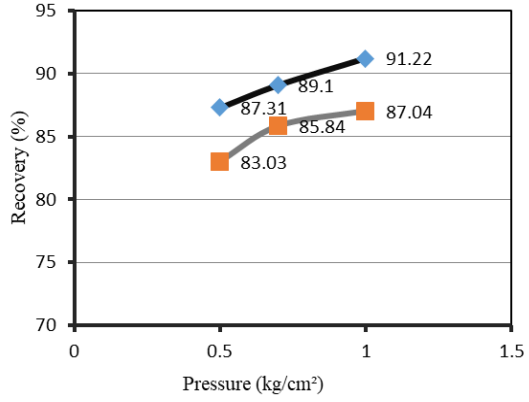

Figure 3: Effect of hydrocyclone pressure on P_2O_5 recovery in underflow.

Table 3. Mass balance of the desliming hydrocyclone tests at different feed pressures for sample P1.

Pressure (kg/cm²)	Slimes weight (%)	Underflow weight (%)	Slimes P_2O_5 grade (%)	Underflow P_2O_5 grade (%)	P_2O_5 recovery in underflow (%)
0.5	10.16	89.84	17.91	13.94	87.31
0.7	8.17	91.83	18.99	13.82	89.10
1.0	6.63	93.37	18.27	13.48	91.22

Table 4. Results of preliminary flotation tests for sample P1.

No.	Collector (g/t)	Depressant (g/t)	Desliming Pressure (kg/cm²)	pH	Conc. P_2O_5 (%)	Conc. Fe_2O_3 (%)	Flotation Recovery (%)	Overall Recovery (%)
1	Flo-YS20 (600) + Lina Z80 (80)	Starch (400)	Without	9.5	32.41	12.96	97.87	97.87
2	Flo-YS20 (800) + Lina Z80 (100)	Starch (400)	Without	9.5	30.64	15.84	98.26	98.26
3	ALKE (400) + Dirol (400)	Starch (400)	Without	9.5	29.66	18.92	97.70	97.70
4	ALKE (500) + Dirol (500)	Starch (400)	Without	9.5	28.84	20.76	98.40	98.40
5	Flo-YS20 (600) + Lina Z80 (80)	Starch (800)	Without	9.5	30.95	11.88	98.30	98.30
6	Flo-YS20 (600) + Lina Z80 (80)	Na_2SiO_3 (400)	Without	9.5	27.78	21.77	98.60	98.60
7	Flo-YS20 (600) + Lina Z80 (80)	Na_2SiO_3 (800)	Without	9.5	30.92	17.05	95.86	95.86
8	ALKE (400) + Dirol (400)	Na_2SiO_3 (400)	Without	9.5	30.82	17.25	97.67	97.67
9	Flo-YS20 (600) + Lina Z80 (80)	Starch (400)	Without	10.5	29.94	17.61	98.48	98.48
10	Flo-YS20 (600) + Lina Z80 (80)	Starch (400)	Without	8.5	23.21	36.16	98.07	98.07
11	Flo-YS20 (600) + Lina Z80 (80)	Starch (400)	0.5	9.5	35.86	8.99	95.10	83.03
12	Flo-YS20 (600) + Lina Z80 (80)	Starch (400)	0.7	9.5	35.07	11.14	96.33	85.83
13	Flo-YS20 (600) + Lina Z80 (80)	Starch (400)	1	9.5	34.76	10.42	95.44	87.06
14	Oleic acid (400)	Starch (400)	0.5	9.5	31.74	16.98	94.7	82.68

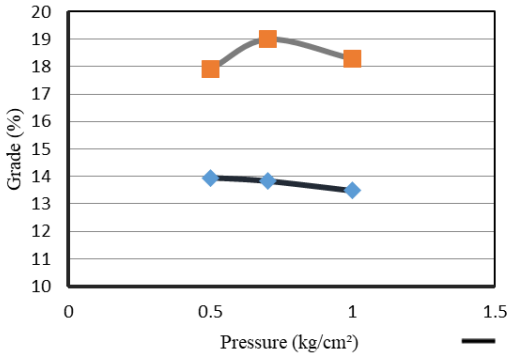

Figure 4: Effect of hydrocyclone pressure on P_2O_5 grade in underflow and slimes.

Based on these results, the hydrocyclone pressure of 0.5 kg/cm² was selected for subsequent flotation tests. Although this pressure resulted in slightly lower recovery (87.31% versus 91.22% at 1.0 kg/cm²), it produced a higher-grade feed for flotation (13.94% P_2O_5) and better simulated the plant operating conditions.

3.3. Flotation optimization for sample P1

3.3.1. Effect of collector dosage

The effect of collector dosage on flotation performance was investigated at pH=9.5 with 400 g/t starch. Figure 5 shows the variation of flotation recovery with collector consumption.

As shown in Figure 5, flotation recovery remained stable (93–95%) when the collector dosage was reduced from 680 to 280 g/t, indicating that the apatite surface in sample P1 can be sufficiently hydrophobized at significantly lower collector concentrations. The plateau suggests that critical surface coverage is achieved at approximately 280 g/t, and further addition does not enhance recovery. A sharp decline to 72.26% at 170 g/t implies insufficient collector for adequate surface coverage, likely exacerbated by iron oxide surfaces (47.17% Fe_2O_3) that consume collector. Based on these results, the optimal collector dosage was selected as 280 g/t (Flo-YS20: 250 g/t + Lina Z80: 30 g/t) for sample P1. This represents a 59% reduction compared to the current plant practice of 680 g/t, highlighting a substantial opportunity for reagent cost savings.

3.3.2. Effect of pulp density

The effect of pulp density on flotation performance was investigated at the optimal collector dosage (280 g/t), pH 9.5, and starch dosage (400 g/t). Two pulp densities of 20% and 35% solids were tested. As shown in Table 5, increasing the pulp density from 20% to 35% slightly improved the concentrate grade from 31.89% to 32.41% P_2O_5 and recovery from 91.55% to 93.91%, while Fe_2O_3 grade increased marginally from 7.55% to 10.90%. The relatively minor changes across the tested range indicate that pulp density is not a critical parameter for this ore type within the 20–35% solids range. A pulp density of 35% solids, consistent with plant practice, was selected for subsequent experiments.

3.3.4. Effect of pH

The effect of pH on flotation performance was investigated at the optimal collector dosage (280 g/t) and starch dosage (400 g/t). The results are presented in Table 6. As shown, increasing pH from 8.5 to 9.5 improved recovery from 92.61% to 94.98%, while the concentrate grade remained relatively stable (32.45% vs. 31.89% P_2O_5). This improvement can be attributed to enhanced collector adsorption on apatite surfaces at near-neutral to slightly alkaline conditions, where the surface charge of apatite favors interaction with anionic collectors. At pH 9.5, the concentrate contained 7.55% Fe_2O_3, indicating effective depression of iron oxides by starch. A further increase to pH 10.5 resulted in a slight improvement in recovery (96.77%), but caused a significant decrease in P_2O_5 grade (30.10%) and a notable increase in Fe_2O_3 grade (12.72%). This reduced selectivity at higher pH is likely due to competitive adsorption of hydroxyl ions and the activation of iron oxide surfaces which promotes collector adsorption on gangue minerals. The optimum pH for selective flotation of apatite from iron oxides in sample P1 was therefore determined to be 9.5.

3.3.4. Effect of starch dosage

As shown in Figure 6, increasing starch dosage up to 400 g/t significantly reduced Fe_2O_3 grade from 16.16% to 7.55%, while P_2O_5 recovery remained above 97%. This indicates that starch molecules selectively adsorb onto iron oxide surfaces through hydrogen bonding and chemical interactions with Fe sites, thereby preventing collector adsorption and subsequent flotation of iron-bearing minerals. The relatively constant recovery in this range suggests that starch does not interfere with apatite flotation at dosages up to 400 g/t, demonstrating its selectivity as a depressant for this ore type. However, a further increase to 500 g/t resulted in a notable decline in recovery to 93.48%, implying that excess starch begins to adsorb onto apatite surfaces as well, causing over-depression of the valuable mineral. The optimum starch dosage for sample P1 was therefore determined to be 400 g/t.

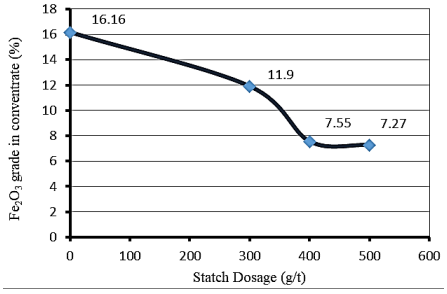

Figure 6. Effect of starch dosage on Fe_2O_3 grade and flotation recovery for sample P1.

3.3.5. Cleaning stages

After optimizing the rougher flotation conditions, the rougher concentrate was subjected to cleaning stages to improve the final concentrate grade. Two sets of experiments were conducted: 1) cleaning without desliming, and 2) cleaning with desliming.

.

Table 5. Effect of pulp density on flotation performance for sample P1.

Pulp Density (% solids)	Conc. Weight (%)	P_2O_5 Grade (%)	Fe_2O_3 Grade (%)	Flotation Recovery (%)
20	35.22	31.89	7.55	91.55
35	34.97	32.41	10.90	93.91

Table 6. Effect of pH on flotation performance for sample P1.

pH	Conc. Weight (%)	P_2O_5 Grade (%)	Fe_2O_3 Grade (%)	Flotation Recovery (%)	Overall Recovery (%)
8.5	38.22	32.45	7.95	92.61	80.86
9.5	40.56	31.89	7.55	94.98	82.93
10.5	44.65	30.10	12.72	96.77	84.49

Cleaning without desliming produced a concentrate with 37.60% P_2O_5 and 4.56% Fe_2O_3 at 93.02% recovery. However, the Fe_2O_3 content remained above the acceptable limit, and froth collection times were significantly extended (7–8 minutes per stage) due to the presence of ultrafine particles.

Cleaning with desliming significantly improved performance. As shown in Table 7, one cleaning stage increased P_2O_5 grade to 37.63% with 5.12% Fe_2O_3, achieving flotation and overall recoveries of 87.43% and 77.21%, respectively. Additional starch (100 g/t) in the cleaning stage had only a minor effect on reducing Fe_2O_3 content (from 5.12% to 4.95%), indicating that starch is more effective in the rougher stage. Two cleaning stages yielded a final concentrate with 40.81% P_2O_5 and 1.74% Fe_2O_3, with flotation and overall recoveries of 80.53% and 70.31%, respectively. The substantial reduction in Fe_2O_3 from 7.55% (rougher concentrate) to 1.74% after two cleaning stages indicates that successive cleaning effectively removes iron-bearing gangue particles entrained in the froth. It should be noted that the actual recoveries are higher than reported, as the cleaner tailings are recycled to the rougher circuit. Based on these results, two cleaning stages were selected as optimal for sample P1.

3.4. Flotation optimization for sample P2

3.4.1. Desliming results

Before flotation optimization, sample P2 was deslimed at the optimal hydrocyclone pressure determined for sample P1 (0.5 kg/cm²). The results are presented in Table 8.

Desliming removed approximately 13 wt.% of the feed as slimes, with the slime fraction containing only 9.52% P_2O_5. In contrast to sample P1, the underflow exhibited higher P_2O_5 grade (13.46%) than the slime fraction (9.52%), indicating that clay minerals and other gangue in sample P2 are preferentially concentrated in the fine fraction. This behaviour is consistent with the mineralogical composition of P2, which contains significant amounts of clay minerals (10.6% montmorillonite) that are softer and more readily ground to ultrafine sizes.

3.4.2. Effect of collector dosage

The effect of collector dosage on flotation performance for sample P2 was investigated at pH 9.5 with 400 g/t starch. The results are presented in Figures 7 and 8.

As shown in Figure 7, flotation recovery decreased sharply from 95.96% to 86.16% when the collector dosage was reduced from 790 g/t (Flo-YS20: 700 g/t + Lina Z80: 90 g/t) to 680 g/t (600 + 80 g/t). This contrasts with sample P1, where recovery remained stable over a wide range of collector dosages. The higher collector demand for P2 can be attributed to the presence of clay minerals (10.6% montmorillonite), which have high surface areas and consume significant amounts of collector through adsorption. A further reduction to 460 g/t caused a substantial drop in recovery to 70.45%. Correspondingly, as shown in Figure 8, the tailings P_2O_5 grade increased from 3.16% to 6.09%, confirming insufficient collector for adequate surface hydrophobization. At the lowest tested dosage (400 g/t), recovery plummeted to 32.66%, with tailings grade reaching 11.51% P_2O_5. This sharp, threshold-like decline contrasts with the gradual plateau observed for sample P1 (Figure 5) and is attributed to the high specific surface area of the montmorillonite present in P2: collector is consumed non-selectively by physical adsorption and slime coating on the clay fraction before it can chemisorb onto apatite calcium sites, so recovery falls abruptly once the available collector can no longer saturate both the clay and apatite surfaces simultaneously, rather than declining gradually as in P1, where iron oxide gangue competes for collector to a lesser extent. Based on these results, the collector dosage of 680 g/t (Flo-YS20: 600 g/t + Lina Z80: 80 g/t) was selected as optimal for sample P2.

3.4.3. Effect of pH

The effect of pH on flotation performance for sample P2 was investigated at the optimal collector dosage (680 g/t) and starch dosage (400 g/t). According to Figure 9, increasing pH from 8.5 to 9.5 significantly improved recovery from 63.66% to 86.16%. This improvement can be attributed to enhanced collector adsorption on apatite surfaces at near-neutral to slightly alkaline conditions where the surface charge of apatite favors interaction with anionic collectors. A further increase to pH 10.5 resulted in a slight improvement in recovery (91.08%).

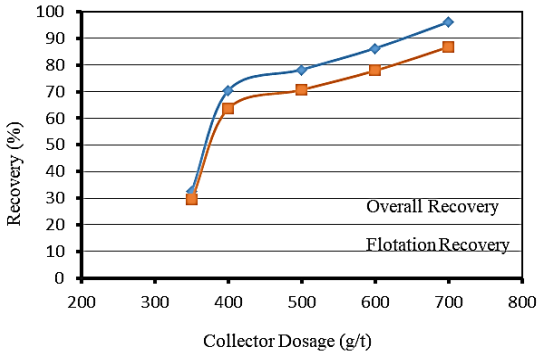

Figure 7. Effect of collector dosage on flotation recovery for sample P2.

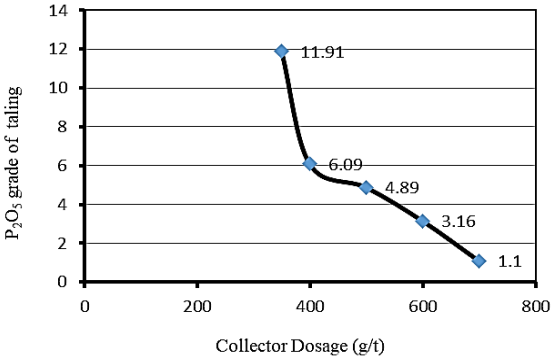

Figure 8. Effect of collector dosage on tailings P_2O_5 grade for sample P2.

However, as can be observed in Figure 10, the concentrate P_2O_5 grade increased from 27.50% at pH 8.5 to 30.63% at pH 9.5, but decreased to 25.38% at pH 10.5, indicating reduced selectivity at higher pH. This is likely due to competitive adsorption of hydroxyl ions and activation of gangue surfaces which promotes collector adsorption on non-valuable minerals. The optimum pH for selective flotation of apatite from sample P2 was therefore determined to be 9.5, consistent with the optimal pH found for sample P1.

3.4.4. Effect of starch dosage

The effect of starch dosage on flotation performance for sample P2 was investigated at the optimal collector dosage (680 g/t) and pH 9.5, with the results summarized in Table 9. Increasing starch dosage from 250 to 400 g/t improved P_2O_5 grade from 28.00% to 30.81% while reducing Fe_2O_3 grade from 7.26% to 4.58%, confirming that starch effectively depresses iron oxides by adsorbing onto their surfaces and preventing collector attachment. However, flotation recovery decreased from 94.24% to 89.77% over the same range, suggesting that some apatite loss occurs as starch dosage increases. It is evident from Table 9 that a further increase to 500 g/t resulted in only a marginal improvement in Fe_2O_3 grade (4.28%) but caused a notable drop in recovery to 86.16%, implying over-depression of apatite at higher starch concentrations. Based on these results, the optimal starch dosage for sample P2 was determined to be 400 g/t, providing the best balance between concentrate grade and recovery.

3.4.5. Cleaning stages

After optimizing the rougher flotation conditions for sample P2, the rougher concentrate was subjected to two cleaning stages to improve the final concentrate grade, following the same approach as for sample P1. As is apparent from Table 10, two cleaning stages improved the P_2O_5 grade from 30.81% to 31.05% while substantially reducing Fe_2O_3 from 4.58% to 2.11%. This confirms that the cleaning stages effectively remove iron-bearing gangue particles from the froth concentrate. However, the improvement in P_2O_5 grade was relatively modest compared to sample P1 (which increased from 31.89% to 40.81%), indicating that the lower initial grade and higher clay content of sample P2 limit the final concentrate quality achievable through cleaning. The flotation recovery decreased from 89.77% to 71.38%, and the overall recovery, accounting for phosphate loss in the slimes, was 64.56%. Based on these results, two cleaning stages were selected as optimal for sample P2, consistent with the approach used for sample P1.

3.5. Blending optimization

3.5.1. Blend 50:50 (P1:P2)

To evaluate the effect of feed blending on flotation performance, a blend consisting of equal proportions (50 wt.% P1 + 50 wt.% P2) was prepared and tested under various conditions. This ratio was selected to assess the maximum allowable contribution of the lower-grade, clay-bearing P2 ore without severely compromising flotation performance.

Flotation experiments were conducted to optimize the key parameters for the blend. As shown in Figure 11, recovery remained above 88% when the collector dosage was reduced from 790 to 570 g/t (Flo-YS20: 500 g/t + Lina Z80: 70 g/t), but dropped sharply to 53.34% at 460 g/t, indicating insufficient collector coverage. The collector demand for the blend (570 g/t) was intermediate between P1 (280 g/t) and P2 (680 g/t), confirming that blending reduces collector consumption compared to processing P2 alone. The optimum pH and starch dosage were found to be 9.5 and 400 g/t, respectively, consistent with the individual ore tests. The rougher concentrate was subjected to two cleaning stages to improve the final concentrate grade. As presented in Table 11, two cleaning stages increased the P_2O_5 grade from 31.45% to 33.00% while significantly reducing Fe_2O_3 from 6.54% to 1.70%, with a flotation recovery of 62.61% and an overall recovery of 55.64%.

3.5.2. Blend 70:30 (P1:P2)

A second blend comprising 70 wt.% P1 and 30 wt.% P2 was prepared to evaluate whether reducing the proportion of the clay-bearing P2 ore would improve flotation performance while still utilizing this lower-grade material. Flotation optimization for the 70:30 blend followed the same procedure as the individual ores. According to Figure 12, the Fe_2O_3 grade in the concentrate decreased as the collector dosage was reduced, with the optimal grade achieved at 460 g/t (Flo-YS20: 400 g/t + Lina Z80: 60 g/t). As shown in Figure 13, recovery remained above 86% at this dosage, while a further reduction to 400 g/t caused a slight decrease in recovery, indicating that 460 g/t provides sufficient collector coverage.

The collector demand for this blend (460 g/t) was lower than both the 50:50 blend (570 g/t) and P2 alone (680 g/t), confirming that increasing the proportion of P1 reduces collector consumption. The optimum pH and starch dosage remained 9.5 and 400 g/t, respectively, consistent with all previous tests. The results of two-stage cleaning are presented in Table 12. Two cleaning stages improved the P_2O_5 grade from 29.12% to 35.26% while reducing Fe_2O_3 from 7.68% to 2.08%, with a flotation recovery of 63.82% and an overall recovery of 56.32%. Although the 70:30 blend achieved a notably higher concentrate grade than the 50:50 blend (35.26% vs. 33.00% P_2O_5), its flotation recovery was only marginally higher (63.82% vs. 62.61%), a difference smaller than the reported recovery reproducibility (±1.5%). This is discussed further in section 4.

Table 7. Effect of cleaning stages on concentrate quality for sample P1.

Cleaning Stages	Conc. Weight (%)	P_2O_5 Grade (%)	Fe_2O_3 Grade (%)	Flotation Recovery (%)	Overall Recovery (%)
No cleaning	38.22	31.89	7.55	97.05	84.73
One stage (without starch)	31.38	37.63	5.12	87.43	77.21
One stage (with starch)	30.74	37.21	4.95	87.40	76.31
Two stages	26.39	40.81	1.74	80.53	70.31

Table 8. Desliming results for sample P2.

Product	Weight (%)	P_2O_5 Grade (%)	CaO Grade (%)	P_2O_5 Recovery (%)
Overflow	13.00	9.52	19.62	9.56
Underflow	87.00	13.46	54.13	90.44

Table 9. Effect of starch dosage on flotation performance for sample P2.

Starch Dosage (g/t)	Conc. Weight (%)	P_2O_5 Grade (%)	Fe_2O_3 Grade (%)	Flotation Recovery (%)	Overall Recovery (%)
250	49.07	28.00	7.26	94.24	85.23
400	40.39	30.81	4.58	89.77	81.18
500	39.10	30.63	4.28	86.16	77.92

Table 10. Effect of cleaning stages on concentrate quality for sample P2.

Cleaning Stages	Conc. Weight (%)	P_2O_5 Grade (%)	Fe_2O_3 Grade (%)	Flotation Recovery (%)	Overall Recovery (%)
No cleaning	40.39	30.81	4.58	89.77	81.18
Two stages	27.86	31.05	2.11	71.38	64.56

Table 11. Effect of cleaning stages on concentrate quality for Blend 50:50.

Cleaning Stages	Conc. Weight (%)	P_2O_5 Grade (%)	Fe_2O_3 Grade (%)	Flotation Recovery (%)	Overall Recovery (%)
No cleaning	36.95	31.45	6.54	87.02	77.34
Two stages	22.01	33.00	1.70	62.61	55.64

Table 12. Effect of cleaning stages on concentrate quality for Blend 70:30.

Cleaning Stages	Conc. Weight (%)	P_2O_5 Grade (%)	Fe_2O_3 Grade (%)	Flotation Recovery (%)	Overall Recovery (%)
No cleaning	38.44	29.12	7.68	86.86	76.65
Two stages	21.72	35.26	2.08	63.82	56.32

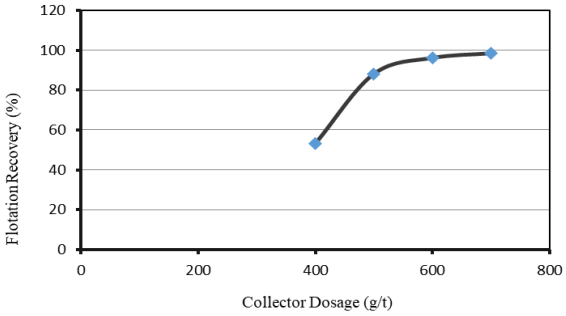

Figure 11. Effect of collector dosage on flotation recovery for Blend 50:50

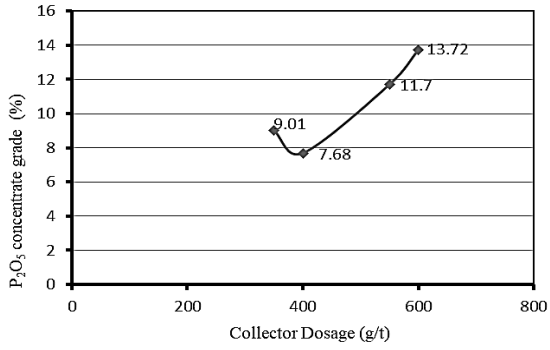

Figure12. Effect of collector dosage on Fe_2O_3 grade for Blend 70:30.

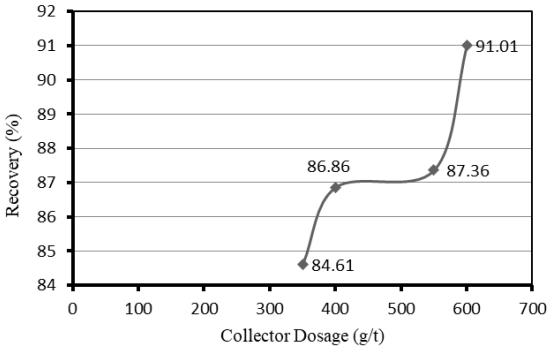

Figure 13. Effect of collector dosage on flotation recovery for Blend 70:30.

4. Discussion

4.1. Comparison with previous studies

The collector reduction achieved for sample P1 in this study (280 g/t, a 59% reduction relative to current plant practice) is broadly consistent with reagent savings reported for other igneous and mixed phosphate ores once ore-specific optimization is applied. Aleksandrova and Elbendari [30] similarly demonstrated the effectiveness of ore-type-resolved anionic flotation for a magmatic phosphate ore, achieving a concentrate of 39.15% P_2O_5 at 94.19% recovery for a lower-grade feed (10.88% P_2O_5) through targeted reagent conditioning rather than blending. The P1 grade achieved in the present study (40.81% P_2O_5) is comparable, while the recovery (80.53%) is lower, a difference attributed to the additional two-stage cleaning applied here to meet a stricter Fe_2O_3 specification rather than to a difference in collector chemistry.

The blending strategy evaluated here parallels, at concentrator scale, the geometallurgical domaining approach described by Tiu et al. [29] for managing feed variability in complex ores in which mineralogically or texturally distinct domains are characterized independently and then combined or scheduled to stabilize plant feed. Whereas Tiu et al. [29] addressed variability primarily through mine-planning-level domain scheduling, the present results show that comparable stabilization can be achieved directly at the Esfordi concentrator through controlled blending of two mineralogically defined ore types, without requiring changes to mine sequencing. This distinction clarifies that the contribution of the present work lies not in the blending concept itself, which is well established in the broader geometallurgy literature, but in its concrete demonstration and quantification for this specific igneous phosphate deposit—a gap that, to the authors' knowledge, has not previously been addressed for Esfordi-type ore.

Considered together, the grade–recovery outcomes for P1 (40.81% P_2O_5, 80.53% recovery), P2 (31.05%, 71.38%), and the 50:50 and 70:30 blends (33.00%/62.61% and 35.26%/63.82%, respectively) trace a consistent trend of increasing concentrate grade with increasing P1 proportion, at the cost of recovery falling below the P1-only value once P2 is introduced into the feed. Constructing a complete grade–recovery curve from a wider set of blend ratios, as suggested during review, would allow this trend to be quantified more rigorously and is recommended as a direct extension of the present work.

4.2. Surface chemistry mechanisms

Although this study did not include zeta-potential, FTIR, or XPS measurements, the collector-adsorption behavior observed for P1 and P2 can be interpreted in light of established mechanistic studies of oleate-type collectors on calcium-bearing minerals. Using ex-situ FTIR internal reflection spectroscopy, Lu et al. [40] showed that oleate chemisorbs onto calcium sites at the apatite surface at pH=9.5, forming an approximately monolayer coverage before excess collector precipitates as calcium oleate; this is consistent with the plateau in P1 recovery observed here between 280 and 680 g/t collector (Figure 5) which suggests that near-monolayer coverage of the apatite surface is achieved well below current plant dosage.

Free and Miller [41] further showed, for the analogous fluorite–oleate system, that collector colloids and precipitated calcium-oleate species can adsorb non-selectively onto gangue surfaces once solution concentration exceeds a critical threshold, offering a plausible mechanism for the elevated Fe_2O_3 pickup observed in P1 concentrates at higher pH (Table 6).

For sample P2, the sharp recovery decline described above is consistent with non-selective consumption of collector by montmorillonite whose high specific surface area and permanent layer charge favor physical adsorption and slime coating rather than the calcium-mediated chemisorption that governs apatite floatability [9, 40]. Distinguishing quantitatively between slime coating, increased pulp viscosity, and preferential entrainment of clay into the froth would require zeta-potential measurements and SEM/EDX analysis of the flotation products which was beyond the scope of the present laboratory-scale study (see Limitations, below).

4.3. Statistical considerations for blend performance

The concentrate grade advantage of the 70:30 blend over the 50:50 blend (35.26% vs. 33.00% P_2O_5) was accompanied by only a marginal recovery difference (63.82% vs. 62.61%) which falls within the reported recovery reproducibility of the duplicate tests (±1.5%) and should therefore be regarded as not statistically distinguishable from zero. The 70:30 blend is nonetheless considered the more favorable condition, since it achieves a materially higher grade at an equivalent recovery. A plausible explanation for the grade increase not translating into a proportional recovery gain is the higher Fe_2O_3 content contributed by the larger proportion of P1 in the 70:30 blend: iron-oxide particles entrained in the froth, or associated changes in froth stability from the higher iron-oxide load, may offset part of the recovery benefit that would otherwise be expected from the larger proportion of the more floatable P1 ore. Confirmatory replicate testing, ideally supported by a factorial or response-surface design, would be needed to establish whether this trend is robust.

4.4. Limitations

Several limitations should be acknowledged. First, flotation conditions were optimized using a one-factor-at-a-time approach; interaction effects between pH, collector, and starch dosage were not explicitly captured, and a response-surface design (e.g., Box–Behnken) could provide a more robust optimum, particularly for the blended feeds, and is recommended as future work. Second, no water chemistry analysis or temperature control was performed in this study; both are known to influence apatite floatability and would be expected to vary under plant conditions. Third, mineral characterization was limited to optical microscopy and XRD; SEM/EDX analysis of the flotation products would be needed to directly confirm the distribution of clay minerals between concentrate and tailings and to distinguish between the competing mechanisms discussed above. Finally, all tests were conducted at laboratory scale (1.0 L cell); scale-up validation would be required before the reagent savings and blending ratios identified here are adopted in continuous plant operation.

5. Conclusion

This study systematically investigated the flotation behaviour of two mineralogically distinct ore types from the Esfordi igneous phosphate deposit and evaluated feed blending as a practical approach for managing ore variability. The following conclusions were drawn:

Mineralogical composition exerts a strong influence on flotation performance. The iron-rich apatite ore (P1) exhibited superior flotation performance, producing a concentrate containing 40.81% P_2O_5 and 1.74% Fe_2O_3 at 80.53% recovery while requiring only 280 g/t collector. This represents a 59% reduction in collector consumption compared with current plant practice. In contrast, the clay-bearing green phosphate ore (P2) required substantially higher collector dosage (680 g/t) and yielded a lower-grade concentrate (31.05% P_2O_5 and 2.11% Fe_2O_3) at 71.38% recovery. The poorer flotation response of P2 was attributed mainly to the presence of clay minerals which increased reagent consumption and reduced flotation selectivity.

Feed blending is an effective operational strategy for mitigating ore variability. Among the tested blending ratios, the 70:30 (P1:P2) blend provided the most favorable balance between concentrate quality, recovery, and reagent consumption, producing a concentrate containing 35.26% P_2O_5 and 2.08% Fe_2O_3 at 63.82% recovery while reducing collector consumption by 32% compared with P2 alone. These results indicate that blending higher-quality and lower-quality ores can improve process stability and facilitate the utilization of variable feed materials without compromising concentrate specifications.

Desliming and two-stage cleaning are essential for achieving high-grade concentrates. Desliming at 0.5 kg/cm² hydrocyclone pressure removed fine gangue particles and improved flotation feed quality for both ore types. Two cleaning stages without additional reagents significantly reduced iron oxide contamination and enhanced concentrate grade.

Optimum flotation conditions were established for each ore type and blend. The optimal conditions consisted of pH=9.5 and a starch dosage of 400 g/t for all samples while collector dosage varied according to ore type and blending ratio, reflecting the strong influence of mineralogical characteristics on reagent demand.

Overall, the findings highlight the value of integrating mineralogical characterization, flotation optimization, and feed blending strategies to improve the processing efficiency of heterogeneous phosphate ores. This approach provides a practical framework for reducing reagent consumption, maintaining concentrate quality, and enhancing resource utilization at the Esfordi phosphate concentrator.

Implications for plant practice. The 59% collector reduction identified for sample P1 applies specifically to feed streams dominated by P1-type ore. Because current plant practice (680 g/t) reflects a naturally mixed feed rather than pure P1, the achievable plant-wide reduction will vary with the instantaneous P1:P2 ratio and should not be assumed to apply uniformly across all feed conditions. In practice, operators could use routine XRF-based feed characterization (e.g., Fe_2O_3 and P_2O_5 grade, used here as a proxy for ore type) to estimate the incoming P1:P2 ratio in near real time and adjust collector dosage and blending ratio accordingly—targeting the 70:30 (P1:P2) ratio identified in this study when sufficient P1-type ore is available, and reserving higher collector dosages for periods when the feed is dominated by the clay-bearing P2 ore. Such a feed-responsive dosing strategy could substantially reduce reagent costs relative to a uniform; worst-case dosage applied regardless of instantaneous feed composition.

It should also be noted that the recovery difference between the 50:50 and 70:30 blends (62.61% vs. 63.82%) is smaller than the reported test reproducibility (±1.5%) and is therefore not statistically distinguishable; the preference for the 70:30 blend rests on its higher concentrate grade at an equivalent recovery, as discussed in section 4.3, rather than on a statistically confirmed recovery improvement.

References

[1]. Pufahl, P. K., & Groat, L. A. (2017). Sedimentary and igneous phosphate deposits: formation and exploration: an invited paper. Economic Geology, 112(3), 483-516. https://doi.org/10.2113/econgeo.112.3.483.

[2]. National Minerals Information Center, 2025, Mineral Commodity Summaries 2025 - PHOSPHATE ROCK Data Release: U.S. Geological Survey data release, https://doi.org/10.5066/P13XCP3R.

[3]. Wills, B. A., & Finch, J. (2015). Wills' mineral processing technology: an introduction to the practical aspects of ore treatment and mineral recovery. Butterworth-heinemann.

[4]. Sis, H. İ. K. M. E. T., & Chander, S. (2003). Reagents used in the flotation of phosphate ores: a critical review. Minerals Engineering, 16(7), 577-585. 10.1016/S0892-6875(03)00131-6

[5]. Aleksandrova, T., Elbendari, A., & Nikolaeva, N. (2022). Beneficiation of a low-grade phosphate ore using a reverse flotation technique. Mineral Processing and Extractive Metallurgy Review, 43(1), 22-27. https://doi.org/10.1080/08827508.2020.1806834.

[6]. Zhang, P., Yu, Y., & Bogan, M. (1997). Challenging the “Crago” double float process II. Amine-fatty acid flotation of siliceous phosphates. Minerals engineering, 10(9), 983-994. https://doi.org/10.1016/S0892-6875(97)00078-2

[7]. Feng, D., & Aldrich, C. (2004). Influence of operating parameters on the flotation of apatite. Minerals Engineering, 17(3), 453-455. https://doi.org/10.1016/j.mineng.2003.10.014

[8]. Sis, H. İ. K. M. E. T., & Chander, S. (2003). Improving froth characteristics and flotation recovery of phosphate ores with nonionic surfactants. Minerals engineering, 16(7), 587-595. https://doi.org/10.1016/S0892-6875(03)00137-7

[9]. Liu, Z., Li, L., Li, Z., Wang, M., Liu, F., & Mi, H. (2025). Review of Interfacial Regulation of Apatite Flotation. Minerals, 15(6), 558. https://doi.org/10.3390/min15060558

[10]. Ding, Z., Li, J., Yuan, J., Yu, A., Wen, S., & Bai, S. (2023). Insights into the influence of calcium ions on the adsorption behavior of sodium oleate and its response to flotation of quartz: FT-IR, XPS and AMF studies. Minerals Engineering, 204, 108437. https://doi.org/10.1016/j.mineng.2023.108437

[11]. Karlkvist, T., Patra, A., Rao, K. H., Bordes, R., & Holmberg, K. (2015). Flotation selectivity of novel alkyl dicarboxylate reagents for apatite–calcite separation. Journal of colloid and interface science, 445, 40-47.

https://doi.org/10.1016/j.jcis.2014.11.072

[12]. dos Santos, M. A., Santana, R. C., Capponi, F., Ataíde, C. H., & Barrozo, M. A. (2012). Influence of the water composition on the selectivity of apatite flotation. Separation Science and Technology, 47(4), 606-612. https://doi.org/10.1080/01496395.2011.621159

[13]. Owens, C. L., Nash, G. R., Hadler, K., Fitzpatrick, R. S., Anderson, C. G., & Wall, F. (2019). Apatite enrichment by rare earth elements: A review of the effects of surface properties. Advances in colloid and interface science, 265, 14-28. https://doi.org/10.1016/j.cis.2019.01.004

[14]. Lu, Y., Drelich, J., & Miller, J. D. (1998). Oleate adsorption at an apatite surface studied by ex-situ FTIR internal reflection spectroscopy. Journal of Colloid and Interface Science, 202(2), 462-476. https://doi.org/10.1006/jcis.1998.5466

[15]. Lu, Y., Drelich, J., & Miller, J. D. (1997). Wetting of francolite and quartz and its significance in the flotation of phosphate rock. Minerals Engineering, 10(11), 1219-1231. https://doi.org/10.1016/S0892-6875(97)00108-8

[16]. Free, M. L., & Miller, J. D. (1996). The significance of collector colloid adsorption phenomena in the fluorite/oleate flotation system as revealed by FTIR/IRS and solution chemistry analysis. International Journal of Mineral Processing, 48(3-4), 197-216. https://doi.org/10.1016/S0301-7516(96)00027-0

[17]. Lan, S., Shen, P., Zheng, Q., Qiao, L., Dong, L., & Liu, D. (2024). Effective flotation separation of apatite from dolomite using a new eco-friendly depressant gallic acid. Green Chemistry, 26(3), 1627-1636. https://doi.org/10.1039/d3gc03325b

[18]. Jong, K., Han, Y., & Ryom, S. (2017). Flotation mechanism of oleic acid amide on apatite. Colloids and Surfaces A: Physicochemical and Engineering Aspects, 523, 127-131. https://doi.org/10.1016/j.colsurfa.2016.11.038

[19]. Cheng, R., Li, C., Liu, X., & Deng, S. (2017). Synergism of octane phenol polyoxyethylene-10 and oleic acid in apatite flotation. Physicochemical Problems of Mineral Processing, 53(2), 1214-1227. http://dx.doi.org/10.5277/ppmp170241

[20]. Cao, Q., Luo, B., Wen, S., & Cheng, J. (2017). Influence of synergistic effect between dodecylamine and sodium oleate on improving the hydrophobicity of fluorapatite. Physicochemical Problems of Mineral Processing, 53(1), 42-55. http://dx.doi.org/10.5277/ppmp170104

[21]. Aarab, I., Amari, K. E., Yaacoubi, A., Etahiri, A., & Bacaoui, A. (2023). Optimization of the flotation of low-grade phosphate ore using DOE: a comparative evaluation of fatty acid formulation to sodium oleate. Mining, Metallurgy & Exploration, 40(1), 95-108. https://doi.org/10.1007/s42461-022-00706-w

[22]. Farid, Z., Abdennouri, M., Barka, N., & Sadiq, M. H. (2022). Grade-recovery beneficing and optimization of the froth flotation process of a mid-low phosphate ore using a mixed soybean and sunflower oil as a collector. Applied Surface Science Advances, 11, 100287. https://doi.org/10.1016/j.apsadv.2022.100287

[23]. Quast, K. (2017). An investigation of the flotation minimum in the oleate flotation of hematite under alkaline conditions. Minerals Engineering, 113, 71-82. https://doi.org/10.1016/j.mineng.2017.08.002

[24]. Bai, S., Li, J., Bi, Y., Yuan, J., Wen, S., & Ding, Z. (2023). Adsorption of sodium oleate at the microfine hematite/aqueous solution interface and its consequences for flotation. International Journal of Mining Science and Technology, 33(1), 105-113. https://doi.org/10.1016/j.ijmst.2022.09.012

[25]. Anzoom, S. J., Bournival, G., & Ata, S. (2024). Coarse particle flotation: A review. Minerals Engineering, 206, 108499. https://doi.org/10.1016/j.mineng.2023.108499

[26]. Kromah, V., Powoe, S. B., Khosravi, R., Neisiani, A. A., & Chelgani, S. C. (2022). Coarse particle separation by fluidized-bed flotation: A comprehensive review. Powder Technology, 409, 117831. https://doi.org/10.1016/j.powtec.2022.117831

[27]. Huang, X., & Zhang, Q. (2023). Interaction behavior between coarse and fine particles in the reverse flotation of fluorapatite and dolomite. Langmuir, 39(36), 12931-12943. https://doi.org/10.1021/acs.langmuir.3c02117

[28]. Drzymala, J. (1994). Characterization of materials by Hallimond tube flotation. Part 1: maximum size of entrained particles. International Journal of Mineral Processing, 42(3-4), 139-152. https://doi.org/10.1016/0301-7516(94)00036-0

[29]. Tiu, G., Ghorbani, Y., Jansson, N., Wanhainen, C., & Bolin, N. J. (2023). Quantifying the variability of a complex ore using geometallurgical domains. Minerals Engineering, 203, 108323. https://doi.org/10.1016/j.mineng.2023.108323

[30]. Tiu, G., Ghorbani, Y., Jansson, N., & Wanhainen, C. (2021). Tracking silver in the Lappberget Zn-Pb-Ag-(Cu-Au) deposit, Garpenberg mine, Sweden: Towards a geometallurgical approach. Minerals Engineering, 167, 106889. https://doi.org/10.1016/j.mineng.2021.106889

[31]. Aleksandrova, T. N., & Elbendari, A. M. (2021). Increasing the efficiency of phosphate ore processing using flotation method. Записки Горного института, 248, 260-271. https://doi.org/10.31897/PMI.2021.2.10

[32]. Talebi, E., Maleki, H., Langari, S., Noaparast, M., Shafaei, S. Z., & Jozanikohan, G. (2026). Comparative Evaluation of Different Collector–Depressant Systems Application in the Reverse Flotation of Apatite and Collophane from a Sedimentary Phosphate Ore Sample. Results in Engineering, 110544. https://doi.org/10.1016/j.rineng.2026.110544

[33]. Jami, M. (2005). Geology, geochemistry and evolution of the Esfordi phosphate-iron deposit, Bafq area, Central Iran (Doctoral dissertation, UNSW Sydney). https://doi.org/10.26190/unsworks/17736

[34]. Boomeri, M. (2012). Rare earth minerals in Esfordi magnetite-apatite ore deposit, Bafq district. Scientific Quarterly Journal of Geosciences, 22(85),71-82. https://doi.org/10.22071/gsj.2012.54023

[35]. Rajabzadeh, M. A., Hoseini, K., & Moosavinasab, Z. (2014). Mineralogical and geochemical studies on apatites and phosphate host rocks of Esfordi deposit, Yazd province, to determine the origin and geological setting of the apatite.

[36]. Hosseini, K., & Rajabzadeh, M. A. (2021). Mineralogy, geochemistry, and fluid inclusion microthermometry of apatite and rare earth element minerals in the Esfordi deposit, NE of Bafq, Yazd Province. Journal of Economic Geology, 13(1), 57-84.

[37]. Hosseini, K., Shahpasandzadeh, M., & Moradian Bafghi, M. H. (2022). Origin of Mineralizing Fluids in the Choghart Magnetite-Apatite Deposit, NE of Bafq: Evidence from Mineralogy, Geochemistry, Microthermometry, Stable (OH and OC) and Unstable Isotopes (U-Pb and Nd-Sm). Journal of Economic Geology, 14(1), 109-155. https://dx.doi.org/10.22067/ECONG.2021.67972.1004

[38]. Soltani, F., Abdollahy, M., Javad Koleini, S. M., & Moradkhani, D. (2017). Selection of an appropriate leaching method for light REEs from Esfordi flotation concentrate based on mineral characterization. Journal of the Southern African Institute of Mining and Metallurgy, 117(5), 443-450.

[39]. Dehghani, A., Azizi, A., Mojtahedzadeh, S. H., & Gharibi, K. (2012). Optimizing rougher flotation parameters of the Esfordi phosphate ore. Mineral Processing and Extractive Metallurgy Review, 33(4), 260-268. https://doi.org/10.1080/08827508.2011.584092

[40]. Lu, Y., Drelich, J., & Miller, J. D. (1998). Oleate adsorption at an apatite surface studied by ex-situ FTIR internal reflection spectroscopy. Journal of Colloid and Interface Science, 202(2), 462–476. https://doi.org/10.1006/jcis.1998.5466

[41]. Free, M. L., & Miller, J. D. (1996). The significance of collector colloid adsorption phenomena in the fluorite/oleate flotation system as revealed by FTIR/IRS and solution chemistry analysis. International Journal of Mineral Processing, 48(3–4), 197–216. https://doi.org/10.1016/0301-7516(96)00006-4